Image of a Spherical Black Hole with Thin Accretion Disk

J.-P. Luminet

Groupe d'Astrophysique Relativiste, Observatoire de Paris, Section d'Astrophysique, F-92190-Meudon, France

Summary. Black hole accretion disks are currently a topic of widespread interest in astrophysics and are supposed to play an important role in a number of high-energy situations. The present paper contains an investigation of the optical appearance of a spherical black hole surrounded by thin accretion disk. Isoradial curves corresponding to photons emitted at constant radius from the hole as seen by a distant observer in arbitrary direction have been plotted, as well as spectral shifts arising from gravitational and Doppler shifts. By the results of Page and Thorne (1974) the relative intrinsic intensity of radiation emitted by the disk at a given radius is a known function of the radius only, so that it is possible to calculate the exact distribution of observed bolometric flux. Direct and secundary images are plotted and the strong asymmetry in the flux distribution due to the rotation of the disk is exhibited. Finally a simulated photograph is constructed, valid for black holes of any mass accreting matter at any moderate rate.

Key words: black holes – accretion disks – geometrical optics

1. Introduction

The aim of the present paper is to provide a reply to the question that many people ask themselves about the optical appearance of a black hole.

In order to be visible a black hole has of course to be illuminated, like any ordinary body. One of the simplest possibilities would be for the black hole to be illuminated by a distant localized source which in practise might be a companion star in a loosely bound binary system. A more interesting and observationally important possibility is that in which the light source is provided by an emitting accretion disk around the black hole, such as may occur in a tight binary system with overflow from the primary, and perhaps also on a much larger scale in a dense galactic nucleus. The general problem of the optical appearance of black holes is related to the analysis of trajectories in the gravitational field of black holes. For a spherical, static, electrical field-free black hole (whose external space-time geometry is described by the Schwarzschild metric) this problem is already well known (Hagihara, 1931; Darwin, 1959; for a summary, see Misner et al., 1973 [MTW]). In Sect. 2 we give only a brief outline of it with basic equations, trying to point out the major features which will appear later. All our calculations are done in the geometrical optics approximation (for a study of wave-aspects, see Sanchez, 1977). In Sect. 3 we calculate the apparent shape of circular rings orbiting a non-rotating black hole and the results are depicted in Figs. 5–6. In Sect. 4 we recall the standard analysis by Novikov and Thorne

(1973) of the problem of energy release by a thin accretion disk in a general astrophysical context, focusing attention more particularly on the analytic solution for the surface distribution of energy release that was derived by Page and Thorne (1974) in the limiting case of a sufficiently low accretion rate. In terms of this idealized (but in appropriate circumstances, realistic) model, we calculate the distribution of bolometric flux as seen by distant observers at various angles above the plane of the disk (Figs. 9–11).

2. Image of a Bare Black Hole

Before analyzing the general problem of a spherical black hole surrounded by an emitting accretion disk, it is instructive to investigate a more simple case in which all the dynamics are already contained, namely the problem of the return of light from a bare black hole illuminated by a light beam projected by a distant source. It is conceptually interesting to calculate the precise apparent pattern of the reflected light, since some of the main characteristic features of the general geometrical optics problem are illustrated thereby.

The Schwarzschild metric for a static pure vacuum black hole may be written as:

$$ds^2 = -\left(1-\frac{2M}{r}\right)dt^2 + \left(1-\frac{2M}{r}\right)^{-1}dr^2 + r^2(d\theta^2 + \sin^2\theta d\phi^2) \quad (1)$$

where r, θ, and ϕ are spherical coordinates and the unit system is chosen such that $G=c=1$. M is the relativistic mass of the hole (which has the dimensions of length). In this standard coordinate system the horizon forming the surface of the hole is located at the Schwarzschild radius $r_s = 2M$.

One can take advantage of the spherical symmetry to choose the "equatorial" plane $\theta = \pi/2$ so as to contain any particular photon trajectory under consideration. The trajectories will then satisfy the differential equation:

$$\left\{\frac{1}{r^2}\left(\frac{dr}{d\phi}\right)\right\}^2 + \frac{1}{r^2}\left(1-\frac{2M}{r}\right) = 1/b^2. \quad (2)$$

The second term in the left member can be interpreted as an effective potential $V(r)$, in analogy with the non-relativistic mechanics. The motion does not depend on the photon energy E and on its angular momentum L separately, but only on the ratio $L/E = b$, which is the impact parameter at infinity.

Let the observer be in a direction fixed by the polar angle ϕ_0 in the Schwarzschild metric, at a radius $r_0 \gg M$. The rays emitted by a distant source of light and deflected by the black hole intersect the observer's detector (for example a photographic plate) at a
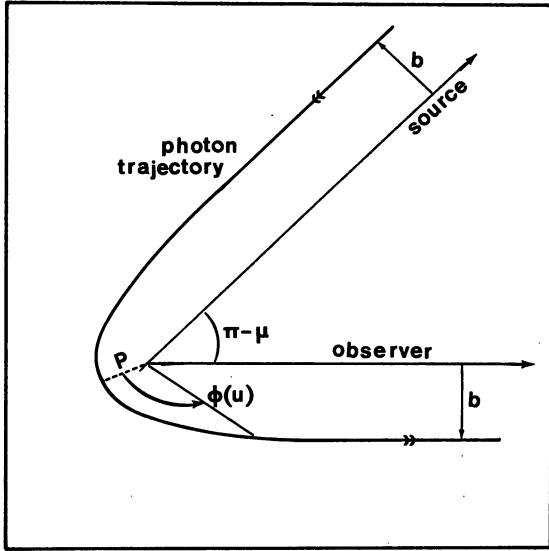
Fig. 1. Trajectory of photons, impact parameter and deflexion angle

distance b from the central point of the plaque. From (2), one sees that a ray with impact parameter b can reach a point at a distance r only if $b \leq \{V(r)\}^{-1/2}$. This is the accessibility condition of the potential barrier. The function $V(r)$ has its maximum at $r_c = 3M$, its value there being $V_c = 1/(27 M^2)$. Therefore, there exists a *critical impact parameter* $b_c = 3\sqrt{3} M$ such that, for $b > 3\sqrt{3} M$, rays are deflected but not captured by the hole, and for $b < 3\sqrt{3} M$, rays are captured.

It is clear that the rim of the "optical" black hole corresponds to rays which are marginally trapped by the black hole: they spiral around many times before reaching the observer, and in our case the rim is located at $b_c = 3\sqrt{3} M = 5.19695$ M. Thus the apparent diameter of the hole is about $10.38 M$.

From this we see that the cross section for the gravitational capture of photons is $\sigma_G = 27 \pi M^2$ (see for instance MTW, Chap. 33; for the expression of the total absorption cross-section of the black hole when wave-aspects are taken into account, see Sanchez, 1977).

Let us return to Eq. (2). Letting $u = 1/r$, we get:

$$(du/d\phi)^2 = 2Mu^3 - u^2 + 1/b^2 \equiv 2MG(u). \tag{3}$$

Let us call u_1, u_2, u_3 the roots of $G(u)$, with $u_1 < u_2 < u_3$ if they are all real. Complete information about the rays is contained in (3), so it is useful to investigate its mathematical structure. It is easy to see that $G(u)$ possesses only one real negative root, and that we have the following possible cases:

$b > b_c : u_1 \leq 0 < u_2 < u_3$

$b = b_c : u_1 = -\dfrac{1}{6M}, \qquad u_2 = u_3 = \dfrac{1}{3M}$

$b < b_c : u_1 \leq 0, u_2,$ and u_3 complex conjugate.

We are interested in orbits that reach the observer's plaque, i.e. for which $b > b_c$. These orbits possess a periastron, and it is convenient to express all the quantities in terms of the periastron distance P, so that if we let: $Q^2 \equiv (P - 2M)(P + 6M)$, we get:

$$u_1 = -\frac{Q - P + 2M}{4MP}, \qquad u_2 = \frac{1}{P}, \qquad u_3 = \frac{Q + P - 2M}{4MP} \tag{4}$$

$$b = P^3/(P - 2M). \tag{5}$$

So, given a value of the periastron, we obtain a value for the impact parameter at infinity, and conversely.

Equation (3) must be integrated over the range of values where u and $G(u)$ are positive, i.e. between u_2 and 0. Figure 1 shows the corresponding trajectory of the ray. We assume that $r_0 \gg M$ is really at infinity (i.e. that the impact parameter on the plate is really b, which is a good assumption), so that the final value, ϕ_∞, of ϕ is given by:

$$\phi_\infty = \frac{1}{\sqrt{2M}} \int_0^{u_2} \frac{dx}{(G(x))^{1/2}}.$$

This integral can be transformed into a classical Jacobian elliptic integral:

$$\phi_\infty = 2(P/Q)^{1/2} \int_{\zeta_\infty}^{\pi/2} (1 - k^2 \sin^2 x)^{-1/2} dx$$

$$= 2(P/Q)^{1/2} \{K(k) - F(\zeta_\infty, k)\}. \tag{6}$$

Here, $K(k)$ is the complete elliptic integral of modulus $k \equiv (Q - P + 6M/2Q)^{1/2}$, $F(\zeta_\infty, k)$ is the elliptic integral of modulus k and argument ζ_∞ such that $\sin^2 \zeta_\infty = (Q - P + 2M)/(Q - P + 6M)$.

The total deviation of the light ray, μ, is given by $\frac{1}{2}\pi + \frac{1}{2}\mu = \phi_\infty$. It is interesting to give the formulas at the limits $P \gg M$ and $P \to 3M$.

For very large P (weak field approximation) we verify immediately that $\mu \sim 4M/P$, $P \sim b$. This famous formula for the deflection of light ray in the gravitational field of a spherical star leads to the Rutherford limit for the differential cross-section $d\sigma/d\Omega = (b/\sin \mu) |db/d\mu|$ (which is precisely the number of particles per unit solid angle $d\Omega = 2\pi \sin \mu d\mu$ collected by the observer), i.e. $d\sigma/d\Omega = (16 M^2)/(\mu^4)$, which is independent of the energy of the incident photons.

For P near the critical value $3M$, i.e. for b near b_c, the asymptotic expansion of elliptic functions for modulus $k \sim 1$ (Gradshteyn and Ryzhik, 1965) leads to the important relation:

$$b = 5.19695 M + 3.4823 M e^{-\mu}. \tag{7}$$

In fact, the particles that come off at a given angle μ include not only those that have really been deflected by μ, also those that have been deflected by $\mu + 2\pi$, $\mu + 4\pi$, ..., $\mu + 2n\pi$, etc. (an infinite series of contributions), and which correspond to the following impact parameters:

$b_0 = b_c + 3.4823 M e^{-\mu}$ (zero circuit)

$b_1 = b_c + 3.4823 M e^{-(\mu + 2\pi)}$ (one circuit)

· · · · ·

$b_n = b_c + 3.4823 M e^{-(\mu + 2n\pi)}$ (n circuits)

· · · · ·

$b_\infty = b_c.$ (infinite circuits).

We see that the nth order contribution to the differential cross section is proportional to

$$db_n/d\mu = -3.4823 M e^{-(\mu + 2n\pi)} \tag{8}$$

thus the total contributions of successive numbers of circuits is proportional to $\sum_0^\infty e^{-2n\pi} = 1/(1 - e^{-2\pi})$. Thus in practise the contribution for $n \geq 2$ is really negligible. We shall see below the observational consequences of this fact.

Once the properties of the deflection angle $\mu(b)$ are known, one is ready to work out what is the image of the black hole illuminated by a parallel beam light, as seen by an observer placed
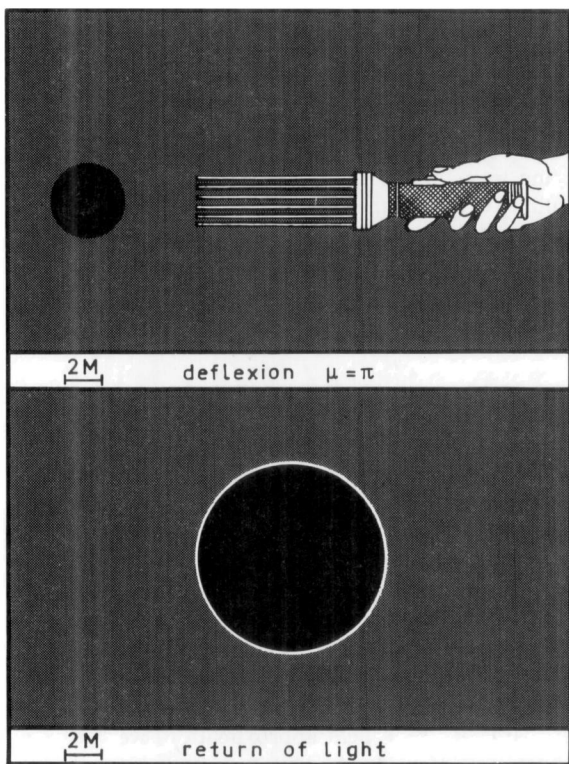
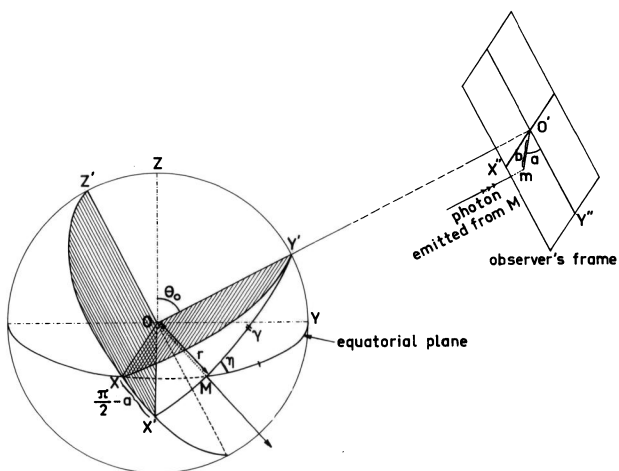**Fig. 2.** Return of light deflected by 180° from a bare black hole

Fig. 3. The coordinate system (see text)

on a Θ-direction. It follows from the above discussion that rays that reach the observer will give a picture consisting of a black disk of radius $b_c = 5.19695\,M$ surrounded by "ghost" rings of different radius and brightness. The exterior ring corresponds to the rays that have not described any circuit; as b approaches its critical value b_c, the rays describe more and more circuits, until in the limit $b_\infty = b_c$ (infinite circuits) the rays are captured.

The external ring is the brightest one; as we see from (8), the brightness decreases exponentially from the external ring to the internal ones.

One can ask for what values of $\Theta = \pi - \mu$ the rings are most visible. It is obvious that, if the observer is placed at an angle Θ

from the direction of incidence close to π, he will not see rings of brightness since almost all the observed photons at small deviations come from large impact parameter, for which circuiting does not take place. In fact, it is clear that the most favourable condition is $\theta = 0$, i.e. the rays are deflected by $\mu = \pi$. Figure (2) gives the corresponding image; the radius of the external ring is $b_1 = 5.341\,M$; this is already near the rim of the black disk of radius $5.197\,M$. The following rings fall at distances even closer, equal respectively to $0.00028\,M$, $0.00000056\,M$, $0.00000000112\,M$, etc.

To conclude this section, the only ring practically distinguishable woud be the external one. This is not only a matter of brightness, but also a matter of resolution.

3. Image of a Clothed Black Hole

Let us now assume that the source of radiation is an emitting accretion disk orbiting around the black hole; the astrophysical properties of such an object will be briefly discussed in the next section. Let the thickness of the disk be negligible with respect to M, so that it is considered as lying in the equatorial plane of the Schwarzschild black hole. The coordinate system is chosen as in Fig. 3. The observer lies in the fixed direction θ_0, $\phi_0 = 0$ (plane YOZ) at a distance $r_0 \gg M$. We consider the disk as an assembly of idealized particles emitting isotropically. Starting from an emitting particle with Schwarzschild coordinates (r, ϕ), a typical trajectory whose asymptotic direction is the observer's direction OO' lies in the plane $OX''Y'$ and reaches the photographic plate (which is the plane $O'X'Y''$) at a point m, determined by its polar coordinates (b, α).

Assuming that the observer is practically at infinity and at rest in the gravitational field of the black hole, then the polar distance from m to $0'$ is precisely the impact parameter of the trajectory, and the polar angle α with the "vertical" direction $O'Y''$ is the complement of the dihedral angle between planes OXY' and $OX'Y'$. For a given coordinate r, varying ϕ from 0 to π (the figure being symmetric with respect to $O'Y''$-axis), we get the apparent shape $b(r) = b(r, \alpha)$ on the photographic plate of the circular ring orbiting the black hole at distance r.

As seen in the previous section, rays emitted from a given point M can circle around the black hole before escaping to infinity, giving an infinite series of images on the photographic plate; the same arguments indicate that only the secundary image (which corresponds to rays that have circuited once) has to be taken into account, images of higher order being almost exactly superposed at the critical value b_c. Thus, for a given emitter M, the observer will detect generally two images, a *direct (or primary) image* at polar coordinates $(b^{(d)}, \alpha)$ and a *ghost (or secundary) image* at $(b^{(g)}, \alpha + \pi)$.

Relationships between the different angles involved by the problem follow directly from the resolution of spherical triangles XMY' and XMX'' (Fig. 3). We get:

$$\cos \alpha = \cot \phi \, \cos \theta_0 / \sin \gamma = \cos \phi \, \cos \theta_0 (1 - \sin^2 \theta_0 \cos^2 \phi)^{-1/2} \tag{9}$$

so that α is a monotonic increasing function of ϕ.

We need also the relation

$$\cos \gamma = \cos \alpha (\cos^2 \alpha + \cot^2 \theta_0)^{-1/2}. \tag{10}$$

Calculation of curves $b^{(d)}(\alpha)$, $b^{(g)}(\alpha)$ at fixed r is performed with a computer. Nervertheless, prior to any precise drawing, we can foresee some characteristic features of the shape of our object by simply considering particular orbits in the plane $\{\phi = 0\}$ for strong inclination ($\theta_0 = 80°$; Fig. 4). Already we can point out that one of
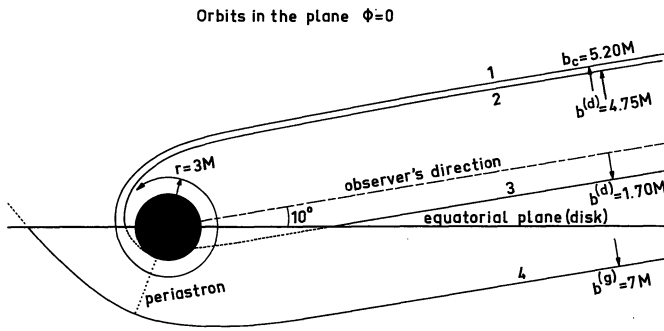
Fig. 4. Illustrative orbits in the plane $\{\phi=0\}$. Trajectory 1 has the critical impact parameter and circles infinitely around the black hole; trajectories 2 and 3 give direct images, trajectory 4 gives a secondary image

the main differences from the problem of the previous section is that not all orbits have necessarily a periastron, or equivalently an impact parameter greater than the critical value b_c. For example, the trajectory 2 is emitted outside the horizon, at a distance $2.60\,M$, and reaches the observer with an impact parameter $b^{(d)}=4.75\,M$, lesser than $b_c=5.20\,M$ (in fact, this trajectory is only theoretically possible, but physically no photon will be emitted so near the horizon, see next section). More significant is the trajectory 3, which is emitted at $r=9.80$ M from the center of the hole but gives a direct image at only $b^{(d)}=1.70$ M. Clearly this is a pure projection effect, already encountered in a newtonian context when one observes Saturn's rings near the equatorial plane. Furthermore, the very small values of $b^{(d)}$ for trajectories emitted at relatively large r but small ϕ imply that the orbits are almost purely radial (indeed trajectory 3 is very close to a straight line); thus, we expect the part of accretion disk between the hole and the observer to give direct images with the aspects of newtonian ellipses which project onto the lower part of the black spot. Figure 4 shows another characteristic feature of the shape: the secondary image is not everywhere in direct juxtaposition to the black spot of radius b_c. In fact, trajectory 4 illustrates how, in order to reach the of radius b_c. In fact, trajectory 4 illustrates how, in order to reach the observer at strong inclination, a photon emitted behind the hole necessarily suffers a weak deviation, and hence has an orbit with large periastron and impact parameter; so, we can presume that the secondary image is really dropped forward the observer's direction (i. e. at relatively small values of ϕ), while on the opposite side it remains crushed around the black spot (at values of ϕ near π).

Now, to get more insight into the mathematics, it is interesting to write down explicitly some algebraic formulas for orbits having a periastron distance P. For the direct image, Eq. (3) leads to:

$$\gamma=\frac{1}{\sqrt{2M}}\int_0^{1/r}(G(x))^{-1/2}dx=2(P/Q)^{1/2}\{F(\zeta_r,k)-F(\zeta_\infty,k)\} \quad (11)$$

where

$$k^2=\frac{Q-P+6M}{2Q},\ \sin^2\zeta_\infty=\frac{Q-P+2M}{Q-P+6M},\ \sin^2\zeta_r$$

$$=\frac{Q-P+2M+4MP/r}{Q-P+6M}. \quad (12)$$

We deduce:

$$\frac{1}{r}=-\frac{Q-P+2M}{4MP}+\frac{Q-P+6M}{4MP}\,\mathrm{sn}^2\left\{\frac{\gamma}{2}\sqrt{P/Q}+F(\zeta_\infty,k)\right\}. \quad (13)$$

Given P, from (10) and (13) we get a relation $r=r(\alpha,P)$, and from (5) we obtain $b^{(d)}=b^{(d)}(r,\alpha)$ for a given angle θ_0.

We can thus draw the *isoradial* curves (corresponding to trajectories emitted at constant coordinate r from the hole) $b^{(d)}=b^{(d)}(\alpha)$ in polar coordinates.

In the newtonian limit, $b=P$ and $\mathrm{sn}\sim\sin$, so that (13) reduces to $b^{(d)}=r\sin\gamma=r(1+\mathrm{tg}^2\,\theta_0\cos^2\alpha)^{-1/2}$, which is obviously the equation of an ellipse of semi-major axis r along $O'X''$ and eccentricity $\sin\theta_0$.

More generally, for the $(1+n)th$ order image, Eq. (11) must be replaced by $2n\pi-\gamma=2(P/Q)^{1/2}\{2K(k)-F(\zeta_\infty,k)-F(\zeta_r,k)\}$ for orbits whose periastron is located between the point of emission and the infinity (that is the case for r slightly greater than $3M$). Of course, here, if the disk is optically thick, a photon whose trajectory intersects the disk would be reabsorbed and will not reach infinity. As we shall discuss later, the realistic physical situation *is* mostly optically thick.

Without taking account of absorption, redshift or physical emissive properties of the disk near the horizon, we have drawn in Figs. 5–6 the direct images of circular rings orbiting at $r=2M$, $r=6M$, $r=10M$, $r=20M$, $r=30M$ and the secundary images for $r=6M$, $r=10M$, $r=30M$ and $r=\infty$, for two values of the inclination angle θ_0.

The qualitative features foreseen above become clearly apparent, specially in Fig. 6; if we superpose newtonian ellipses for corresponding values of r, the curves fit perfectly up to fairly large values of α, of the order of 70°, the deformation becoming drastic only for the part of the ring behind the hole.

In practise, it is clear that, taking account of realistic physical properties of the accretion disk, what we would in fact observe through a telescope would be dramatically different from the mushroom of Fig. 6! The purpose of the following section is to study the actual distribution of flux that would really be observed.

4. Realistic Appearance of a Black Hole Accretion Disk

Until now we have considered the geometrical optics about a theoretical object consisting of a black hole surrounded by a thin accretion disk. It is appropriate at this stage to ask oneself what could be the relevance of such an object in astrophysics.

From an observational point of view, this problem is of importance: since a stationary black hole does not radiate either electromagnetic or gravitational waves, it could be detected only indirectly through its gravitational influence on the ambient medium.

Moreover, with recent discoveries of intense discrete X-ray sources with rapid variability, a considerable interest has focused upon gaz accretion onto compact objects such as neutron stars and black holes, and it is now currently admitted that accretion is probably the main process involved in a larger number of high-energy astrophysical situations, ranging from novae to quasars and other kinds of active galactic nuclei (see for instance Eardley and Press, 1975; Lightman et al., 1975).

Models of black holes with accreting medium are generally considered in the context of black holes in orbit about "normal" stars (binary systems) or supermassive black holes ($M\gtrsim10^7\,M_\odot$) which might reside at the centers of some active galactic nuclei (Lynden-Bell, 1969; Hills, 1975).

In both situations, the accreting matter is likely to have high specific angular momentum, so that the accretion would be far from spherical, but only axisymmetric with the matter flattened in the form of a more or less thin disk.
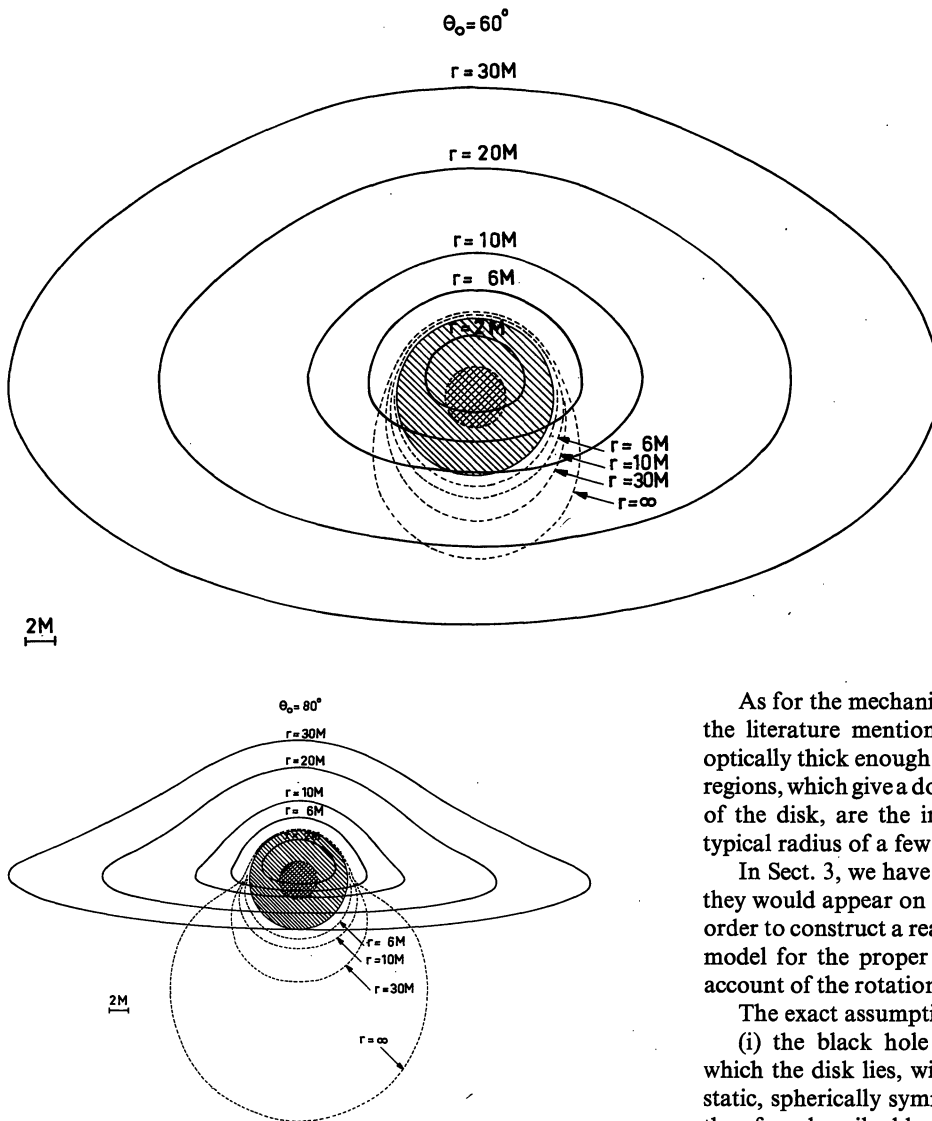
232

$\theta_o = 60°$

r = 30M

r = 20M

r = 10M

r = 6M

r = 6M
r = 10M
r = 30M
r = ∞

2M

Fig. 5. Isoradial curves representing rays emitted at constant radius from the hole, as seen by an observer at 30° above the disk's plane. Full lines: direct images; dashed lines: secundary images

$\theta_o = 80°$

r = 30M

r = 20M

r = 10M

r = 6M

r = 6M
r = 10M

r = 30M

r = ∞

2M

Fig. 6. Isoradial curves as seen by an observer at 10° above the disk's plane

A necessary condition for the existence and stability of a thin disk is to be in *a subcritical regime of accretion*, which may be characterized by an accretion rate $M \lesssim 10^{-8} (M/M_\theta) M_\theta/$yr, for which the intrinsic luminosity of the disk remains far below the critical Eddington luminosity.

The mechanical equilibrium of accreting disks has been first discussed by Prendergast and Burbidge (1968) for accretion onto white dwarfs and by Shakura and Sunyaev (1972), Pringle and Rees (1972), for accretion onto neutron stars and black holes. All these binary models were newtonian; Novikov and Thorne (1973) have calculated the effects of General Relativity on the inner regions of the accreting disk.

For our purpose, two important facts must be noticed. First, the gas can be generally considered as moving along quasi-circular Keplerian orbits with velocity $v_\perp = (M/r^3)^{1/2}$ in the Newtonian region; second, accreting disks around black holes have an inner radius r_{min}, due to relativistic corrections which destabilize circular orbits at r between r_{min} and the horizon. It is well known that $r_{min} = 6M$ in the case of a Schwarzschild black hole.

As for the mechanism of production of radiation by the disk, the literature mentioned above confirms that the disk will be optically thick enough for the radiation to be thermal. The hotter regions, which give a dominant contribution to the total luminosity of the disk, are the inner regions close to the horizon, with a typical radius of a few times M.

In Sect. 3, we have calculated the isoradial curves $r = $const as they would appear on a distant observer's photographic plate. In order to construct a realistic image, we must now choose a precise model for the proper luminosity of the disk, as well as taking account of the rotation of the disk which induces a Doppler shift.

The exact assumptions are the following:

(i) the black hole has an external space-time geometry in which the disk lies, with negligible self-gravity; this geometry is static, spherically symmetric, uncharged and asymptotically flat, therefore described by the Schwarzschild line element (1).

(ii) the disk is geometrically thin, i.e. at radius r its thickness $2h$ is $\ll r$, but nervertheless opaque.

(iii) when averaged the gas elements of the disk move very nearly in equatorial circular geodesic orbits about the black hole.

(iv) Effects such as possible absorption by distant diffuse clouds surrounding the black hole are neglected, as also is the effect of secondary heating of the disk by reabsorption of some of its own light.

For many applications, one can argue that a Kerr geometry would be much more realistic; however, some isoradial curves in a Kerr geometry have been computed by Cunningham and Bardeen (1973) and by Pineault and Roeder (1977), and the results show indeed small deviations with the Schwarzschild case; in fact, the asymmetry of the curves becomes noticeable only for high specific angular momentum of the hole and concerns chiefly the lower part of secondary image, which will in any case be hidden by the frontal direct image of the disk since the rays are supposed to be reabsorbed when they intersect the optically thick disk.

Thus, our calculation with the Schwarzschild geometry may give a very good idea of what would be really observed about a moderately rotating black hole.

An explicit steady-state model for disk around a black hole is obtained in combining equations of vertical structure with
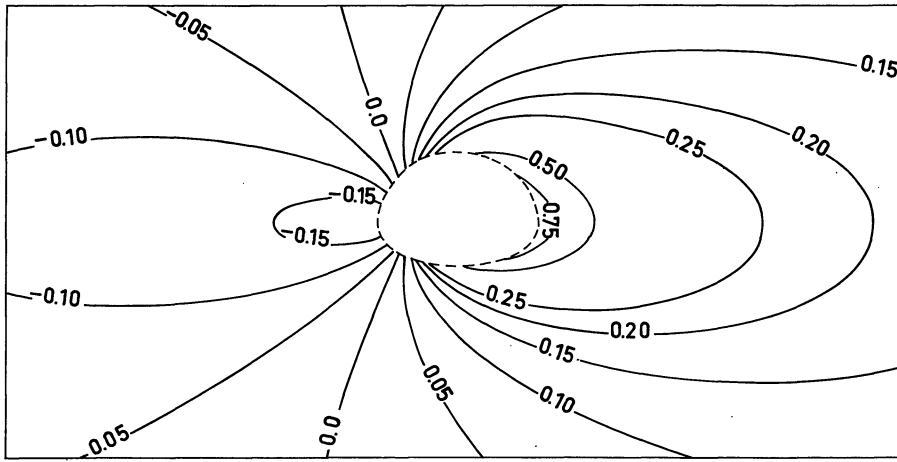
Fig. 7. Curves $\{z=\text{constant}\}$ as seen by an observer at 30° above the disk's plane. Dashed line: the apparent inner edge of the disk

equations of radial structure (see Novikov and Thorne, 1973). The disk can be generally divided in three regions:

(i) an outer region in which gas pressure dominates over radiation pressure and in which the opacity is predominantly free-free.

(ii) a middle region in which gas pressure dominates over radiation pressure but opacity is predominantly due to the electron scattering.

(iii) an inner region in which radiation pressure dominates over gas pressure and opacity is predominantly due to the electron scattering.

For our present purpose which is concerned only with the total (bolometric) brightness distribution, and not with the more detailed spectral appearance, the distinction between these three regions is unimportant (actually for relatively cold disks such as those are expected to be found in binary systems with very small rate or about supermassive hole accreting few gas far below the critical Eddington value, the inner and middle regions may not exist).

In the case of a Schwarzschild black hole, it has been shown by Page and Thorne (1974) that the flux of radiation from the surface of the disk is given simply by:

$$F_S = \frac{3 M \dot{M}}{8 \pi} \frac{1}{(r^*-3)r^{*5/2}} \left[\sqrt{r^*} - \sqrt{6} \right.$$
$$\left. + \frac{\sqrt{3}}{3} \text{Log} \left\{ \frac{(\sqrt{r^*}+\sqrt{3})(\sqrt{6}-\sqrt{3})}{(\sqrt{r^*}-\sqrt{3})(\sqrt{6}+\sqrt{3})} \right\} \right] \quad (15)$$

where $\dot{M}$ is the accretion rate and r^* the radius of the gas element in units of $M (r^*=r/M)$.

The flux is maximum at $r^* \sim 9.55$, for which $(8\pi/3 M \dot{M}) F_{S\,max} \sim 1.146\ 10^{-4}$, and most of the radiation comes from the region between the inner edge $r=6M$ and $r \sim 30M$, which can be considered as the "living core" of our object.

As explained by Ellis (1971), the observed bolometric flux F_0 will differ from the intrinsic flux of the source F_S by the inverse 4th power of the redshift factor $1+z$. The 4th power may be understood as arising from (i) the loss of energy suffered by each photon due to the redshift (one power), (ii) the lower measured rate of arrival of photons due to the time dilatation (one power), and (iii) the relativistic correction to solid-angle measurements (two powers).

Our next step therefore is to calculate the factor $(1+z)$ at each point of the optical image. Since the observer is supposed to have a fairly good resolution, he is close enough to the source to neglect cosmological redshift. Therefore the $(1+z)$-factor will consist of a Doppler part and a gravitational part. For a photon emitted by a source particle orbiting about the black hole the $(1+z)$-factor can be derived as follows: in the rest frame of the emitting particle, the photon has an energy which is the projection of the photon's 4-momentum p on the 4-velocity u of the emitting particle:

$$E_{em} = p_t u^t + p_\phi u^\phi = p_t u^t \left(1 + \Omega \frac{p_\phi}{p_t} \right) \quad (16)$$

where Ω is the angular velocity of the atom about the black hole. The components p_t and p_ϕ of the photon's 4-momentum are conserved along its trajectories; far from the hole, they are the photon's energy E_{obs} and the projection of its angular momentum on the z-axis. The ratio p_ϕ/p_t is nothing but the impact parameter of the photon relative to the z-axis. Thus, by Fig. 3, we shall have:

$$p_\phi/p_t = b \cos \eta = b \sin \theta_0 \sin \alpha. \quad (17)$$

For a quite general stationary axisymmetric metric the redshift of photon will therefore be given by:

$$1+z = E_{em}/E_{obs} = u^t (1 + \Omega b \cos \eta)$$
$$= (1 + \Omega b \cos \eta)(-g_{tt} - 2g_{t\phi} - 2g_{\phi\phi})^{-1/2}.$$

In the Schwarzschild case Ω has the keplerian value $\Omega = (M/r^3)^{1/2}$ and the relevant metric components are given by $g_{t\phi}=0$, $g_{tt} = -(1-2M/r)$, $g_{\phi\phi}=r^2$, so that (18) reduces to the expression:

$$1+z = (1-3M/r)^{-1/2}(1+(M/r^3)^{1/2}b \sin \theta_0 \sin \alpha). \quad (19)$$

Figures 7–8 represent numerically computed curves of constant z on the observer's photographic plate for the direct image, at two values of the inclination angle θ_0. We see in fact that the Doppler blueshift contribution involved by the rotation of the disk in the left half-part of the plate can exceed the overall gravitational redshift part due to the presence of the black hole, so that the corresponding photons have a resulting blueshift. The curves are abruptly cut by the dotted line corresponding to the inner edge of the disk, since no photons are emitted within this limit.

Equation (19) is of course valid also for the secondary image, but we have not depicted the resulting values because part of the
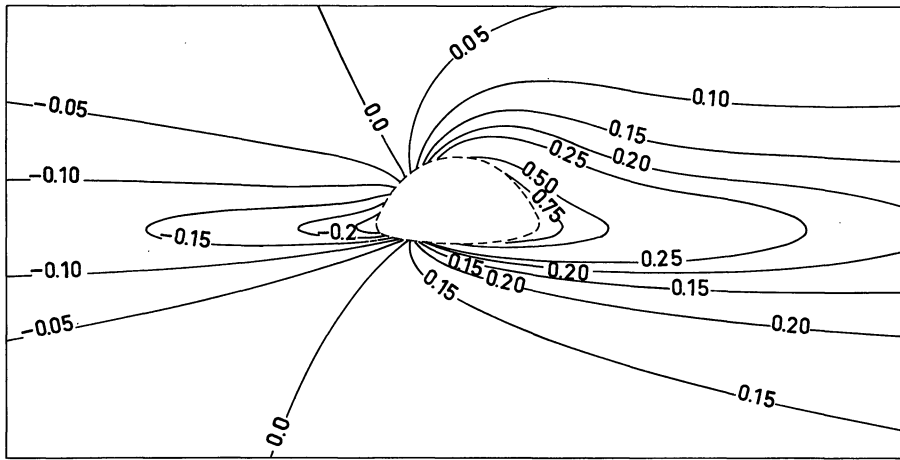
234

Fig. 8. Curves $\{z=\text{constant}\}$ as seen by an observer at 10° above the disk's plane
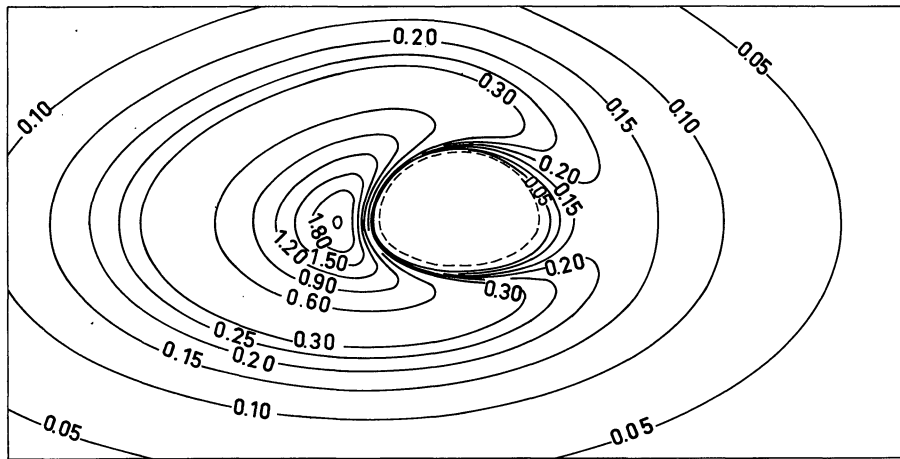

Fig. 9. Curves of constant flux in units of $F_{S\text{max}}$, as senn by an observer at 30° above the disk's plane. Dashed line: the apparent inner edge of the disk (flux = 0)
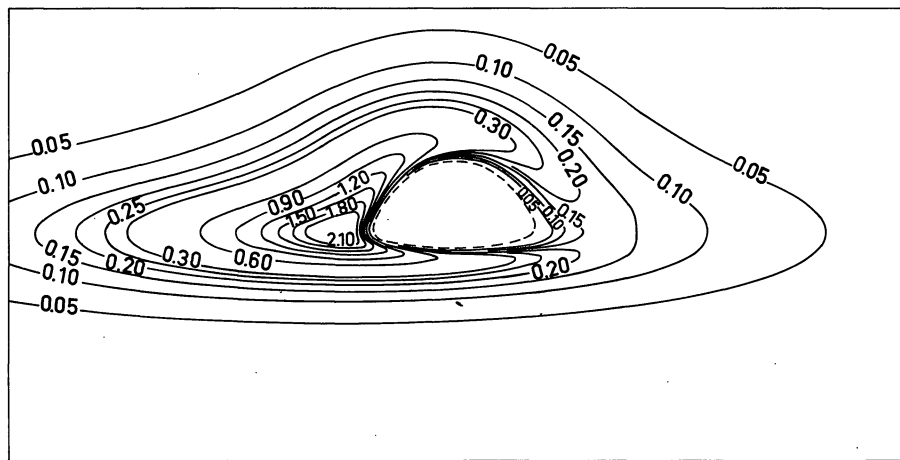

Fig. 10. Curves of constant flux in units of $F_{S\text{max}}$, as seen by an observer at 10° above the disk's plane. The maximum value within the area limited by $F_0=2.10$ is 2.62

secondary image that will be visible (i.e. not reabsorbed by the direct image) reduces to a nearly circular line at impact parameter $b\sim5.25\,\text{M}$, just above the critical value $3\sqrt{3}\,M$ (cf. Fig. 6).

Having calculated the value of z at each point in the observer's photographic plate at polar coordinates (b,α), the observed bolometric flux $F_0=F_S/(1+z)^4$ may be computed relative to a total factor $F_{S\text{max}}$. Figures 9–10 show the curves of constant F_0 as

measured in units of $F_{S\,\text{max}}$ for the direct image and two values of θ_0. The flux is of course maximum in the regions where the spectral shift is a blueshift, occurring at a mean distance corresponding roughly to maximum intrinsic luminosity. Again the flux for the secondary image has not been depicted; a simple way to over-estimate its value along the thin ghost line is to make $r=9.55\,M$ (radius of maximum intrinsic luminosity) and $b=5.25\,M$ (mean
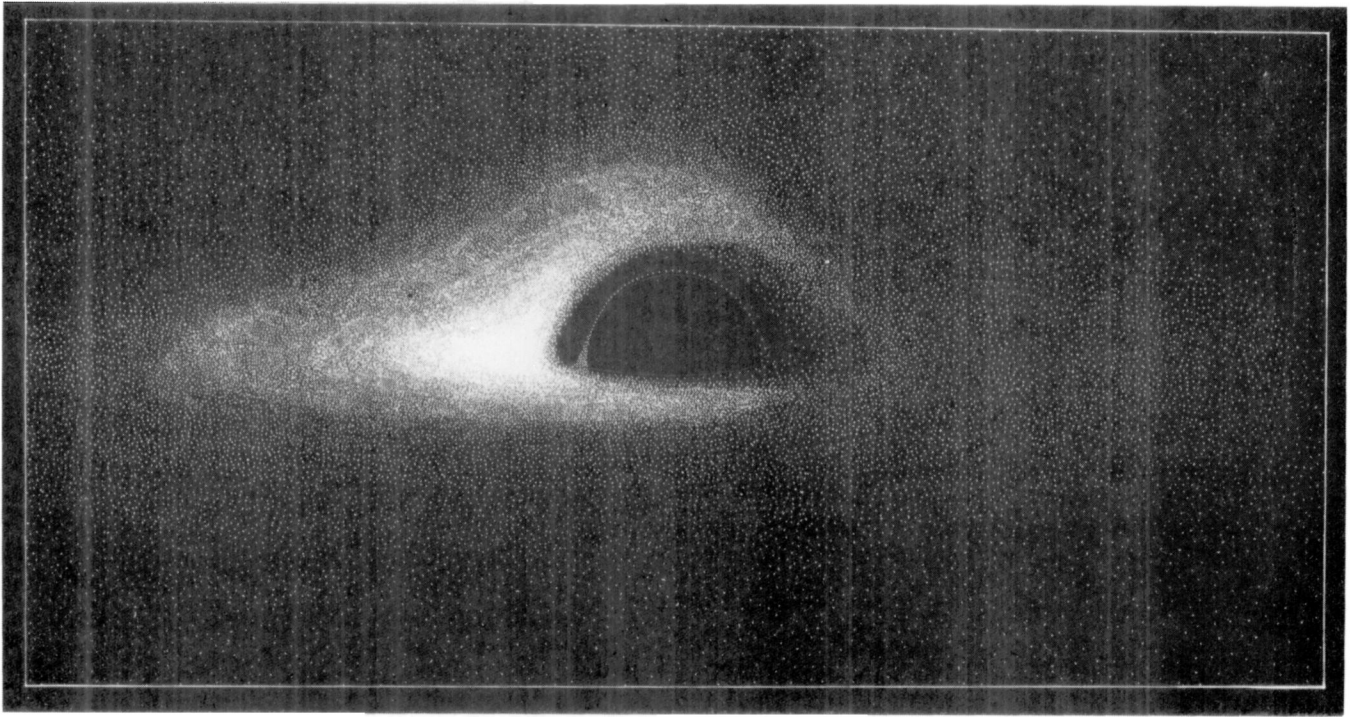
Fig. 11. Simulated photograph of a spherical black hole with thin accretion disk

impact parameter of the visible part of the secundary image) in Eqs. (15) and (19).

The results are taken into account in Fig. 11, which represents the final result of this paper, namely a simulated "bolometric photography" of a static black hole with thin accretion disk.

Figures 9–11 are valid for a large number of black hole situations, i.e. black holes with any mass accreting matter at any rate sufficiently far below the Eddington limit. Thus our picture could represent many relatively weak sources, such as for instance the supermassive black hole whose existence in the nucleus of M 87 has been suggested recently by Young et al. (1978).

It is important to point out that for more spectacular sources such as quasars and Seyfert galaxies, the theory has not yet been developed enough to provide reliable models that could be visualized analogously.

References

Cunningham, C.T., Bardeen, J.M.: 1973, *Astrophys. J.* **183**, 237
Darwin, C.: 1959, *Proc. Roy. Soc. London* A **249**, 180
Eardley, D.M., Press, W.H.: 1975, *Ann. Rev. of Astron. Astrophys.* **13**, 381
Ellis, G.F.R.: 1971, Relativistic Cosmology in *General Relativity and Cosmology*, ed. R. Sachs, Academic Press, New York
Gradshteyn, I.S., Ryzhik, I.W.: 1965, Table of Integral Series and Products, Academic Press, New York
Hagihara, Y.: 1931, *Japan. J. Astron. Geophys.* **8**, 67
Hills, J.G.: 1975, *Nature* **254**, 295
Lightman, A.P., Rees, M.J., Shapiro, S.L.: 1975, Accretion onto compact objects, Lectures at the Enrici Fermi School, Varenna, Italy, July 1975
Lynden-Bell, D.: 1969, *Nature* **223**, 690
Misner, C.W., Thorne, K.S., Wheeler, A.J.: 1973, Gravitation, Freeman, San Francisco
Novikov, I.D., Thorne, K.S.: 1973, in *Black Holes*, Les Houches, ed. DeWitt and DeWitt, Gordon and Breach, New York
Page, D.N., Thorne, K.S.: 1974, *Astrophys. J.* **191**, 499
Prendergast, K.H., Burbidge, G.R.: 1968, *Astrophys. J. Letters* **151**, L 83
Pringle, J.E., Rees, M.J.: 1972, *Astron. Astrophys.* **21**, 1
Pineault, S., Roeder, R.C.: 1977, *Astrophys. J.* **212**, 541
Shakura, N.I., Sunyaev, R.A.: 1973, *Astron. Astrophys.* **24**, 337
Sanchez, N.: 1977, Phys. Rev. **D16**, 937; 1978, to appear
Young, P.J., Westphal, J.A., Kristian, J., Wilson, C.P., Landauer, F.P.: 1978, *Astrophys. J.* **221**, 721